



Universiteit  
Leiden  
The Netherlands

## **Development of novel strategies to regenerate the human kidney**

Leuning, D.G.

### **Citation**

Leuning, D. G. (2018, July 3). *Development of novel strategies to regenerate the human kidney*. Retrieved from <https://hdl.handle.net/1887/63486>

Version: Not Applicable (or Unknown)

License: [Licence agreement concerning inclusion of doctoral thesis in the Institutional Repository of the University of Leiden](#)

Downloaded from: <https://hdl.handle.net/1887/63486>

**Note:** To cite this publication please use the final published version (if applicable).

Cover Page



Universiteit Leiden



The handle <http://hdl.handle.net/1887/63486> holds various files of this Leiden University dissertation.

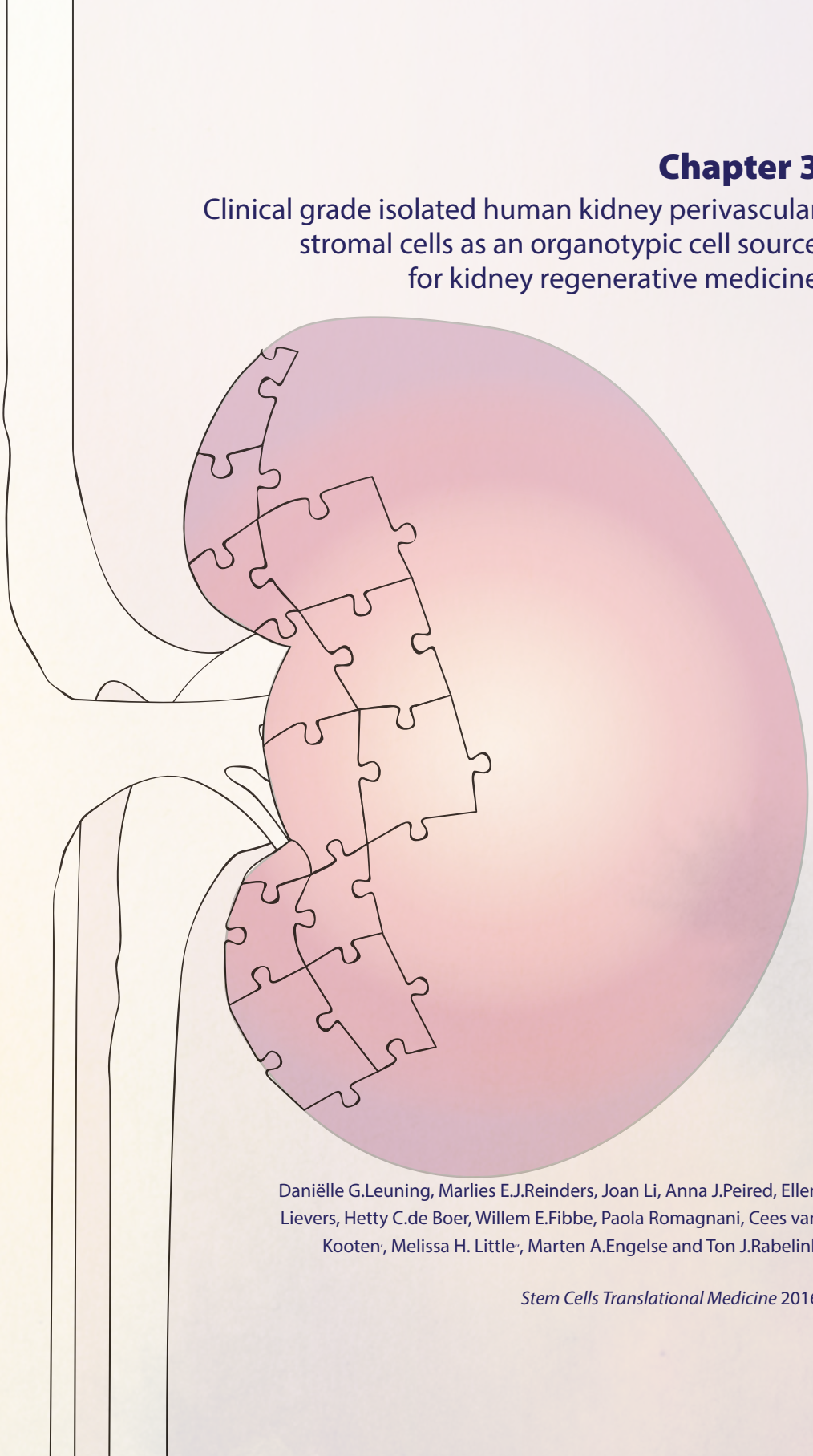
**Author:** Leuning, D.G.

**Title:** Development of novel strategies to regenerate the human kidney

**Issue Date:** 2018-07-03

## Chapter 3

### Clinical grade isolated human kidney perivascular stromal cells as an organotypic cell source for kidney regenerative medicine



Daniëlle G. Leuning, Marlies E.J. Reinders, Joan Li, Anna J. Peired, Ellen Lievers, Hetty C. de Boer, Willem E. Fibbe, Paola Romagnani, Cees van Kooten, Melissa H. Little, Marten A. Engelse and Ton J. Rabelink

*Stem Cells Translational Medicine* 2016

## Abstract

Mesenchymal stromal cells (MSCs) are immunomodulatory and tissue homeostatic cells that have shown beneficial effects in kidney diseases and transplantation. Perivascular stromal cells (PSCs) identified within several different organs share characteristics of bone marrow derived MSC (bmMSCs). These PSCs may also possess tissue-specific properties and play a role in local tissue homeostasis. We hypothesised that human kidney-derived PSCs (hkPSCs) would elicit improved kidney repair compared to bmMSCs. Here we introduce a novel, clinical grade isolation method of hkPSCs from cadaveric kidneys by enriching for the perivascular marker, NG2. hkPSCs show strong transcriptional similarities to bmMSCs, but also show organotypic expression signatures, including the HoxD10 and HoxD11 nephrogenic transcription factors. Comparable to bmMSCs, hkPSCs showed immunosuppressive potential and, when co-cultured with endothelial cells, vascular plexus formation was supported which was specifically in the hkPSCs accompanied by an increased NG2 expression. hkPSCs did not undergo myofibroblast transformation after exposure to TGF $\beta$ , further corroborating their potential regulatory role in tissue homeostasis. This was further supported by the observation that hkPSCs induced accelerated repair in a tubular epithelial wound scratch assay which was mediated through HGF release. *In vivo*, in a neonatal kidney injection model, hkPSCs re-integrated and survived in the interstitial compartment, while bmMSCs did not show this potential. Moreover, hkPSCs gave protection against the development of acute kidney injury *in vivo* in a model of rhabdomyolysis mediated nephrotoxicity. Overall, this suggests a superior therapeutic potential for the use of hkPSCs and/or their secretome in the treatment of kidney diseases.

## Introduction

Mesenchymal stromal cells (MSCs) are immune modulatory and anti-fibrotic cells originally isolated from the bone marrow (bmMSCs) and are characterized by their spindle shaped morphology and ability to adhere to plastic. bmMSCs are able to differentiate into fat, bone and cartilage and express the stromal markers CD73, CD90 and CD105 while being negative for CD34 and CD45.<sup>1,2</sup> In several experimental models of kidney disease (among others cisplatin, glycerol and ischemia-induced injury), MSC treatment enhanced tissue repair and reduced fibrosis.<sup>3,4</sup> In a transplantation model, MSC therapy could prolong graft survival and a regulatory T-cell dependent tolerance was observed.<sup>5</sup> These promising results led to the first clinical trials with bmMSCs in renal transplantation. Although the group sizes were small and the studies were mainly set up to show safety and feasibility of MSC therapy, the first results suggest an immunomodulatory effect of bmMSC therapy.<sup>6-9</sup>

Previously it has been shown that perivascular stromal cells with characteristics similar to bmMSCs exist within many different solid organs, including skeletal muscle, pancreas, adipose tissue and placenta.<sup>10</sup> Due to the perivascular location of these cells, close interaction is possible with several cell types, including endothelial cells, epithelial cells, resident macrophages, dendritic cells and recruited inflammatory cells. Therefore, these cells are most likely important for tissue homeostasis and control of repair processes and inflammation.<sup>11</sup>

MSC-like cells could also be isolated from murine kidneys based on Sca-1 expression. These renal Sca1<sup>+</sup>Lin<sup>-</sup>CD45<sup>-</sup> cells showed a unique phenotype and immunomodulatory potential.<sup>12-14</sup> Murine kidney colony forming cells (kCFU-F) were also Sca-1<sup>+</sup> and although these kCFU-F have a comparable stromal marker expression and trilineage differentiation potential compared to bmMSCs, there is a distinct gene and protein expression profile.<sup>15</sup> This suggests that although kCFU-F and bmMSCs may look similar, functionally there may be differences. Li et al. showed that these cells are indeed different from bmMSCs. In particular the cell fraction isolated based on expression of HoxB7, a collecting duct marker, was able to undergo epithelial-to-mesenchymal transition and upon delivery into neonatal mice kidneys these cells integrated back into the collecting duct while bmMSCs lacked this capacity.<sup>16</sup>

We hypothesized that perivascular stromal cells can also be isolated from the human kidney (hkPSCs) in a clinical grade manner and that these cells have tissue-specific functions. Extensive characterization of hkPSCs, both *in vitro* and *in vivo*, show a capacity for these cells to stabilize endothelial cells, reduce renal injury and support tubular repair. The latter to a greater extent than bmMSCs, suggesting indeed organotypic properties.

## Materials and Methods

### Isolation and expansion of clinical grade human kidney derived perivascular stromal cells

Cells were isolated from human transplant grade kidneys discarded for surgical reasons using clinical grade protocols, enzymes and products. For all kidneys a research consent was given and the study was approved by the local medical ethical committee and the ethical advisory board of the consortium.

Kidneys were flushed with UW cold storage solution (Bridge to life, Elkhorn, Wisconsin, US) containing heparin (Leo Pharma, Ballerup, Denmark) directly after surgery and stored on ice. Within 30 hours kidneys were flushed again with UW and the perirenal fat and kidney capsule were removed. The renal artery was cannulated and the kidney was perfused via a pump driven (Masterflex Applikon, Schiedam, the Netherlands) recirculation system at 37 degrees with DMEM-F12 (Lonza) at 300ml/min. . Afterwards the kidney was perfused with collagenase (2500 units, NB1, Serva) and DNase (2,5 ml Pulmozyme, Genentech) at 37°C with a flow of 300ml/min. After approximately 30 minutes, the tissue was digested and after gentle massage the resulting cell suspension was collected and washed in DMEM-F12 containing 10% fetal calf serum. Cells were then either directly put into culture or frozen in liquid nitrogen. The complete standard operation procedure (SOP) for the isolation procedure can be found in Supplementary file 1.

Kidney cell suspensions were cultured in alphaMEM (Lonza, Verviers, Belgium) containing 5% platelet lysates, glutamine (Lonza, Basel, Switzerland) and penicillin/streptomycin (Lonza) and cells were cultured in tissue culture flasks until confluency was reached. At passage 1 cells were trypsinized and NG2 cell enrichment was performed using MACS according to manufacturer's protocol (Miltenyi Biotech, Gladbach, Germany). The NG2 positive fraction was cultured in aMEM containing 5% platelet lysate. The cultures were maintained at 37°C and 5% carbon dioxide. Half of the medium was refreshed twice a week. When the cells reached confluence, the cells were collected using trypsin (Lonza) and re-plated at  $4 \times 10^3$  cells/cm<sup>2</sup>. Experiments were performed with FACS confirmed homogeneous NG2 positive hkPSCs between passages 4-8 cultured in aMEM 5% platelet lysate unless stated differently.

## Isolation and expansion of human bone marrow derived mesenchymal stromal cells

Ethical committee approval and written consent from the donors was obtained for the aspiration of human bone marrow. Heparinized bone marrow was aspirated under local or general anesthesia. The mononucleated cell fraction was isolated by Ficoll density gradient separation and plated in tissue culture flasks at a density of  $160 \times 10^3$  mononucleated cells/cm<sup>2</sup> in alphaMEM (Lonza) supplemented with penicillin/ streptomycin (Lonza) and 5% platelet lysate. The cultures were maintained at 37°C, 5% carbon dioxide. Half of the medium was refreshed twice a week. When the MSC colonies or cultures reached confluence, the cells were collected using trypsin (Lonza) and re-plated at  $4 \times 10^3$  cells/cm<sup>2</sup>. Experiments were performed between passages 4-8.

## Morphology and immunophenotype analysis

The expanded cell populations were characterized by morphology (spindle shaped cells) which was imaged with an inverted bright-field microscope (Leica DFC 295). For immunophenotyping, the cells were stained for NG2, PDGFR- $\beta$ , CD146, CD73, CD90, CD105, CD31, CD34, CD45, CD56, HLA class I (ABC) and HLA class II (DR). All specific fluorochrome-labeled antibodies and isotype controls were purchased from BD Bioscience (BD Bioscience, Franklin Lakes, NJ, USA) except for CD105 (Ansell Corporation, Bayport, MN, USA).

## Microarray sample preparation and data analysis

RNA was isolated from biological triplicates using Trizol reagent (Life Technologies, Bleiswijk, the Netherlands) and the RNeasy kit (Qiagen, Heidelberg, Germany) according to the manufacturer's protocol. The quality and quantity of RNA was assessed using a Nanodrop spectrophotometer (Nanodrop Technologies, Wesington, USA) and a Bioanalyzer (Agilent Technologies, Santa Clara USA). Gene expression profiling was performed by Aros Applied Biotechnology (Aarhus, Denmark). cDNA and cRNA synthesis, labeling and subsequent hybridization on the Human HT12 V4 Gene Expression Beadchips (Illumina Inc., San Diego, USA) were performed according to manufacturer's protocols. The beadchips, targeting more than 47000 gene transcripts, were scanned using iSCAN system (Illumina Inc., San Diego, USA) and fluorescence intensities were uploaded into GenomeStudio Software (Illumina Inc, San Diego, USA) Genes with a detection p-value of  $>0.05$  for all samples were excluded. Average signals  $>200$  in either the bmMSCs or hKPSCs were considered above background levels. Subsequent data was quantile normalized and the Pearsons correlation coefficient was calculated ( $r^2$ ). Differential expression was analyzed using the gene expression module of Genome Studio (Illumina). For the table of the top differential expressed genes, genes were sorted on highest diff. score . False discovery rates (FDR) were calculated according to Benjamini and Hochberg for a total number of 8462

transcripts. All genes in the top 5 up- and down-regulated genes showed significant differential expression. For the heatmap in Fig. 3A the delta average signal of bmMSCs vs hkPSCs was set to 200 (which is the threshold of the measurement) and 2600 genes selected were analysed for clustering in R software. Clustering in R software was also performed for 27 homeobox genes. Expression of HoxD10 and HoxD11 was confirmed by Quantitative real-time polymerase chain reaction (QPCR) in duplo of the same biological triplicates. QPCR was performed using iQ SYBR Green Supermix on iCycler realtime detection system (BioRad, Veenendaal, the Netherlands) as per the manufacturer's instructions. The real-time PCR primers of HoxD10 are AGACAGTTGGACAGATCCGAA(fw) and CGAAATGAGTTTGTTCGCGCTTAT (rv) and of HoxD11 TCGACCAGTTCTACGAGGCA (fw), and AAAAAGCTCGCGTTCCAGTTCG (rev). The amplification reaction volume was 12.5  $\mu$ L in total, consisting of 6.25  $\mu$ L iQ SYBR Green PCR master mix, 0.5  $\mu$ L primers, 2.5  $\mu$ L cDNA and 3.25  $\mu$ L water. Messenger RNA (mRNA) level was normalized to the housekeeping gene glyceraldehyde-3-phosphate dehydrogenase (GAPDH).

### Tri-lineage differentiation potential

hkPSCs and bmMSCs were cultured in adipogenic, osteogenic and chondrogenic medium according to the manufactures protocols (Lonza). After 3 weeks of culture, in the adipogenic differentiation assay lipid droplets were stained using Oil Red O and in the osteogenic differentiation assay calcium depositions were stained with Alizarin Red. For chondrogenic differentiation cell pellets were formalin-fixed (4% PFA O/N) and embedded in paraffin. Subsequently 5  $\mu$ m sections were de-paraffinized, rehydrated and stained with 1% toluidine blue for 20 min. All differentiation assays were analysed with an inverted bright-field microscope (Leica DFC 295).

### Cytokine excretion, peripheral blood mononuclear cell isolation and proliferation assay

hkPSCs and bmMSCs of 3 different donors were plated in flat-bottom 96-well plates and after 5 days of culture supernatants were harvested and cytokine expression profiles were determined in the supernatant with the Bio-Plex Human Cytokine 17-Plex Panel following the manufacturer's instructions (Bio-Rad Laboratories, Veenendaal, the Netherlands). Cytokines in culture medium were also measured as a negative control.

Peripheral blood mononuclear cells (PBMCs) were isolated from buffy coats of healthy blood donors by density gradient centrifugation using Ficoll-isopaque and frozen in liquid nitrogen until use. Cultured hkPSCs and bmMSCs (passage 6-8) of 3 different donors were plated in flat-

bottom 96-well plates (Costar, Sigma-Aldrich) and allowed to attach overnight in DMEM-F12 with 10% normal human serum (NHS). Culture in 10% NHS was chosen as platelet lysates are able to suppress PBMC proliferation on their own (data not shown). PBMCs were stimulated with anti-CD3/antiCD28 Dynabeads (Invitrogen) and were seeded in triplicate at a concentration of  $1 \times 10^5$  cells/well. Stromal cells were added to the PBMC proliferation assay in a ratio of 1:4 and 1:8. After 5 days  $^3\text{H}$ -thymidine (0.5 mCi) was added and after 16 hours  $^3\text{H}$ -thymidine incorporation was determined as a measure of proliferation.

### Vascular plexus assay

Human umbilical cords were obtained from the Leiden University Medical Center (Leiden, The Netherlands) after informed consent from the parents.

Human umbilical vein endothelial cells (HUVECs) were isolated according to Jaffe et al<sup>17</sup>, with minor modifications: trypsin/EDTA (Sigma/Aldrich, Steinheim, Germany) was used to enzymatically detach the endothelial cells from the vein and the endothelial cells were cultured on fibronectin-coated flasks (isolated from bovine plasma; Sigma/ Aldrich) and refreshed twice a week with EC-medium consisting of M199 Earl's salt with L-glutamine (Invitrogen, Carlsbad, US), supplemented with 10% (v/v) fetal calf serum (PAA Cell Culture Company), pen/strep (PAA Cell Culture Company, Pasching, Germany) 1000 IU of heparin (Leo Pharma, Ballerup, Denmark) and 25 mg bovine pituitary extract (BPE) (Invitrogen). HUVECs were used at passage 2-3.<sup>17</sup>

Stromal cells and HUVECS were cocultured in a 96-wells plate (Costar, Sigma-Aldrich) for 1 week in a 4:1 ratio as described previously.<sup>18</sup> After 1 week cells were fixated for 10 minutes with ice-cold methanol (100%) and endothelial sprouting was visualized with CD31 immune fluorescence (BD Bioscience, Franklin Lakes, NJ, USA, Zeiss LSM500). The percentage capillary coverage was analyzed with imageJ software. NG2 immunofluorescence (BD Bioscience) was determined (Zeiss LSM500) and quantified as mean fluorescent intensity in image J.

### TGF- $\beta$ stimulation

hkPSCs and bmMSCs were seeded in a density of 200.000 cells in a 6 wells plate and stimulated for 48hours with 10 ng/ml TGF- $\beta$ 1 (preprotech, London, United Kingdom). Cells were subsequently trypsinized, permeabilized with 0.1% saponine and labeled with  $\alpha$ -SMA (BD Bioscience).  $\alpha$ -SMA expression was analyzed with flow cytometry and mean fluorescent intensities were calculated (Kaluza, Beckman Coulter, Indianapolis, USA).

### Kidney epithelial wound scratch assay

hkPSCs and bmMSCs of 3 different donors were plated in a density of 200,000 cells/well in a 6 well culture plate (Costar, Sigma-Aldrich) and cultured for 48 hours. HK2 cells were seeded in PTEC medium consisting of a 1:1 ratio of Dulbecco's modified Eagle's medium and Ham's F-12 (Lonza) supplemented with insulin (5 µg/ml), transferrin (5 µg/ml), selenium (5 ng/ml), hydrocortisone (36 ng/ml), tr-iodothyronine (40 pg/ml) and epidermal growth factor (10 ng/ml) (Sigma-Aldrich) in a density of 500,000 cells/well in a 6 wells cell culture plate (Costar) and cultured until confluent. A scratch wound was created in the monolayer of HK2 cells using a 200 µl pipette tip. After the scratch, cells were washed with PBS and provided either with fresh medium (aMEM 5% PL) or with complete conditioned medium from either hkPSCs or bmMSCs. Scratched were imaged at 4, 7, 14 and 28 hours at the same position in duplicates with an inverted bright-field microscope (Leica DFC 295). The scratch area was measured at each time point using ImageJ software and the percentage wound closure was calculated.

Growth factors in the conditioned medium of kPSCs were measured using a custom made growth factor panel following manufacturer's instruction. (R&D systems, Minneapolis, USA). The HGF-receptor was blocked with an HGF receptor/c-MET antibody (R&D systems) in a concentration of 1 µg/ml 1 hour prior to the wound scratch assay and after adding the hkPSC supernatant. In the control conditions an isotype antibody (goat IgG, homemade) was added.

### Neonatal injection model

Animal experiments were approved by the University of Queensland Animal Ethics Committee and adhered to the Australian Code of Practice for the Care and Use of Animals for Scientific Purposes. Neonates of outbred CD1 mice were used for neonatal injection. hkPSCs and bmMSCs of resp. 3 and 2 different donors were injected into the neonatal kidneys at postnatal day 1 (PND1) using a microinjection pipet in a protocol adapted from the protocol previously described<sup>16</sup>. In short, neonates were anesthetized and a small incision in the skin was made. Cells were re-suspended in PBS and mixed with Fluoresbrite Yellow Green microspheres (2.0 µm; Polyscience) in a ratio of 1:50 for identification of injection sites in the neonatal kidney. Using a Eppendorf microinjector, cells were injected into the kidney through the muscle layer in a volume of 300 nl, corresponding with 3000-5000 cells. Kidneys were harvested at 4 days post-injection. In total 7 mice were analyzed; 3 mice with hkPSCs from 3 different donors; 3 mice with bmMSCs from 2 different donors and 1 sham operated mouse. In all mice, injection into the kidney was confirmed by fluorescence of the co-injected microspheres.

### Glycerol-induced rhabdomyolysis model of acute kidney injury

Animal experiments were performed in accordance with institutional, regional, and state guidelines and in adherence with the Italian National Institutes of Health Guide for the Care and Use of Laboratory Animals. Rhabdomyolysis-induced acute kidney injury was studied in 6-week-old male C57Bl/6 mice ((Envigo RMS Srl, San Pietro al Natisone, Italy) by intramuscular injection on day 0 with hypertonic glycerol (8 ml/kg body weight of a 50% glycerol solution; Sigma-Aldrich) into the inferior hind limbs as described previously.<sup>19</sup> hkPSCs were labeled with the PKH26 Red Fluorescence Cell Linker Kit (Sigma-Aldrich) according to manufacturer's instructions, and labeling efficiency was verified by flow cytometry. Cells were acquired before and after labeling using a MACSQuant Analyzer Flow Cytometer and analyzed with MACSQuantify software (Miltenyi Biotec GmbH, Bergish Gladbach, Germany). Cell vitality was monitored using propidium iodide staining and we observed >95% living cells. The mice received PKH26-labelled hkPSC following one of two injection routes. Subcapsular injection: Four hours following kidney injury, mice (n=6 for BUN measurement, n=4 for confocal microscopy) were anesthetized with Avertin (2,2,2-Tribromoethanol, 250mg/kg, Sigma-Aldrich) and subjected to dorsal incision on the left side to exteriorize the left kidney. A 1-mm incision was made in the capsule of the kidney and 750,000 cells were injected in 25µl of sterile PBS using a Hamilton syringe equipped with a 27G blunt-ended needle. After cell infusion, the kidney capsule was cauterized with an electric scalpel, and the dorsal incision was sutured. The mouse was rehydrated with subcutaneous injection of 500ul saline solution and maintained in a warm environment for 2 hours post-surgery. Control mice were injected saline solution (n=6 for BUN measurement, n=4 for confocal microscopy). Intravenous retro orbital injection: Four hours and 24 hours following kidney injury, mice (n=6 for BUN measurement, n=4 for confocal microscopy) were anesthetized with isoflurane (Aerrane, Baxter, Rome, Italy) and injected retroorbitally through the venous plexus with 750,000 cells in 150 µl of sterile PBS each time using a 27G needle. Control mice were injected saline solution (n=8 for BUN measurement, n=4 for confocal microscopy).

Blood samples were obtained from the submandibular venous sinus at day 0, 4, 6 and 14, and blood urea nitrogen (BUN) levels were measured by Reflotron System (Roche Diagnostics, Rotkreuz, Switzerland). Four animals per group were sacrificed at day 6 and kidney, lungs and liver were harvested for confocal microscopy.

## Immunofluorescence of kidney sections

Neonatal injection model: kidney samples were fixed in 4% PFA followed by 30% sucrose overnight and embedded in TissueTek OCT compound (Sakura Finetek, Torrance, CA). Samples were frozen in liquid nitrogen and stored at -80°C. Ten micrometer thick sections were cut and post-fixed with 4% PFA for 10 minutes at room temperature. Stainings were performed using the manufacturer's protocol (Mouse on Mouse (MOM) kit, Vector labs, Brunswick Chemie, Amsterdam, the Netherlands). Samples were stained with antibodies against human mitochondria, nuclei and collagen IV (Abcam, Cambridge, UK) and analysed using a TCS SP8 laser confocal microscope (Leica, Eindhoven, the Netherlands). Rhabdomyolysis-induced acute kidney injury model: Confocal microscopy was performed on 10 µm sections of renal frozen tissues using a TCS SP5-II laser confocal microscope (Leica, Milan, Italy). Staining for FITC-labeled *Dolichos Biflorus Agglutinin* (DBA) and FITC-labeled *Lotus tetragonolobus* agglutinin (*LTA*) (Vector laboratories, Burlingame, California) was performed following manufacturer's instructions. To-pro-3 (Invitrogen Carlsbad, CA, USA) was used for counterstaining nuclei.

## Statistical analysis

Differences between two groups were analyzed using unpaired two-sample t test. When more than two groups were analysed a two way ANOVA test was used with as posthoc test the Bonferroni's comparison test. Differences were considered statistically significant when  $p < 0.05$ . Data analysis was performed using GraphPad Prism, version 5.0 (Graphpad Prism Software Inc. San Diego, USA). For statistical analysis of the microarray data p-values were corrected for multiple testing according to Benjamini and Hochberg.

## Results

### A novel method to isolate clinical grade human kidney-derived perivascular stromal cells (hkPSCs)

In order to evaluate whether hkPSCs are a potential new cell source for use in cell therapy to treat kidney disease in a clinical setting, we chose to develop a clinical grade acceptable standard operation procedure (SOP) with the use of clinical grade materials and enzymes. This protocol is developed based on the pancreatic islet isolation protocol currently in use for clinical application in our center.<sup>20</sup> Perivascular stromal cells were isolated based on NG2 expression. NG2 is an integral membrane proteoglycan which is associated with perivascular cells during vascular morphogenesis.<sup>21</sup> Within the human kidney, NG2 is mainly expressed around the large

arteries and the afferent and efferent arteriole (Fig 1a). NG2 expression is more restricted than the expression of CD271, an enrichment marker for bmMSCs<sup>22</sup> (Fig 1b) or PDGFR- $\beta$  positive perivascular cells (Fig 1c). These markers are also expressed within the glomeruli and around the peritubular capillaries of the kidney. NG2 positive cells were isolated from a pool of ten transplant-grade kidneys discarded for surgical reasons. Experiments were performed and results are shown for three different donors. The average donor age was 62 years with an average estimated creatinine clearance (Cockcroft) of 105 ml/min. In order to isolate NG2 positive cells, these kidneys were perfused with collagenase to dissociate into single cells, enriched based on plastic adherence then sorted based on NG2 expression at the first passage (Fig 1d).

### Characterization of human kidney derived perivascular stromal cells

NG2 positive hkPSCs showed a bright field morphology similar to bmMSCs (Fig 2a) and, like bmMSCs, were positive for the pericyte markers NG2 and PDGFR- $\beta$  as shown with confocal microscopy (Fig 2b). Growth characteristics are shown from flow cytometry confirmed NG2 homogeneous populations, at around passage 9 hkPSCs reached senescence (Fig 2c). In addition to NG2 hkPSCs were positive for the surface markers PDGFR- $\beta$ , CD146, CD73, CD90, CD105 while being negative for CD31, CD34, CD45 and CD56, as determined by FACS (Fig 2d). This marker expression is robust as depicted by the mean fluorescent intensity (MFI) of cells of three different donors (Fig 2e). Whereas human bmMSCs were able to differentiate into all three lineages, hkPSCs could differentiate towards osteocyte and chondrocyte, while no adipogenic differentiation was observed (biological triplicates) (Fig 2f).

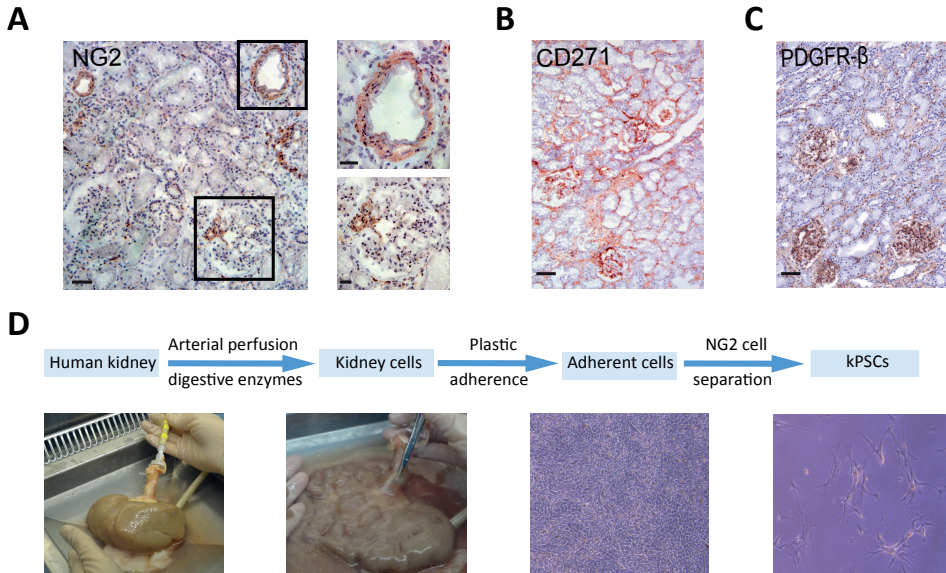


**Figure 1. Isolation method of human kPSCs.** A) NG2 is expressed in the human kidney mainly around the arteries, arterioles and afferent and efferent arterioles of the glomerulus. CD271 (B) and PDGFR- $\beta$  (C) are also expressed within the glomeruli and around the peritubular capillaries. D) Schematic representation of the isolation method. In order to obtain NG2 positive hkPSCs, human kidneys are continuously perfused with digestive enzymes to single kidney cells. Afterwards crude kidney cell suspensions were cultured on plastic for selection on plastic adherence and subsequently sorted for NG2 positivity resulting in the appearance of spindle shaped cells. Scale bars = 50  $\mu$ m (A, left), 20  $\mu$ m (A, right), and 50  $\mu$ m (B, C). Abbreviations: kPSCs, kidney-derived perivascular stromal cells; PDGF-R-b, platelet-derived growth factor-receptor

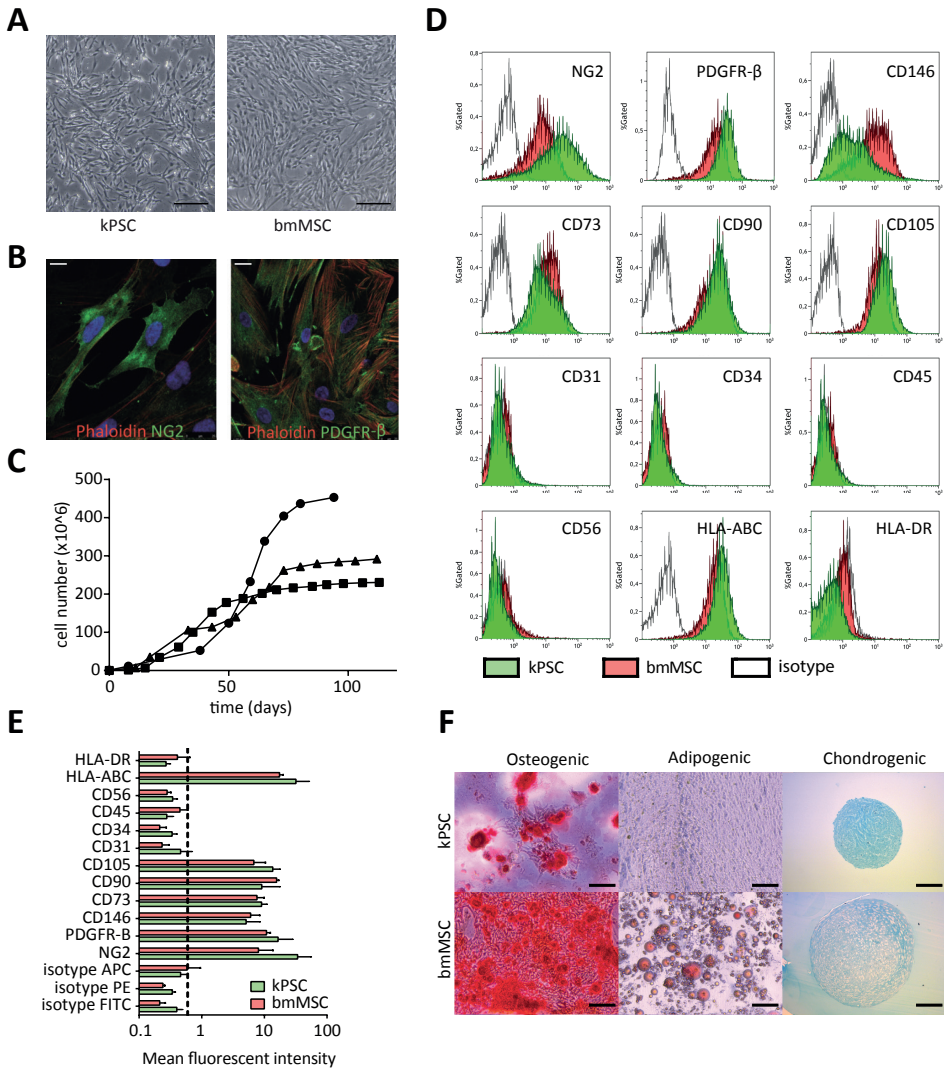


**Figure 2. Characterization of human kPSCs.** A) hkPSCs have a similar morphology compared to bmMSCs and are positive for NG2 and PDGFR-B as shown with confocal images (B). C) Growth characteristics of hkPSCs D) Representative FACS analysis show that hkPSCs are positive for the pericytic markers NG2, PDGFR- $\beta$  and CD146 and the MSC markers CD73, CD90 and CD105 while being negative for CD31, CD34, CD45, CD56. hkPSCs express type I HLA (HLA-ABC) and are negative for type II HLA (HLA-DR). E) Mean fluorescent intensity of the different markers (n=3 donors.) F) Tri-lineage differentiation. hkPSCs differentiate into bone and cartilage but not into adipocytes. Scale bars = 200mm(A, F) and 20mm(B). Abbreviations: BM-MSC, bone marrow-derived mesenchymal stromal cells; FITC, fluorescein isothiocyanate; HLA, human leukocyte antigen; kMSC, kPSC, kidney-derived perivascular stromal cells; PDGF-R-b, platelet-derived growth factor-receptor

### Organ specific gene expression profile of human kidney derived perivascular stromal cells

In order to further compare hkPSCs to bmMSCs, Illumina microarray expression profiling was performed on biological triplicates of different donors. Analysis of expression levels of 35000 transcripts showed that most genes showed a similar expression level (Pearson correlation coefficient of 0,9625) suggesting high similarity between the two cell types (Fig 3a). However, 2600 genes were differentially expressed and hierarchical clustering was able to distinguish based upon cell source (Fig 3b). Table 1 shows the top 5 up and down regulated genes comparing bmMSCs and hkPSCs based on differential p-value. The top 50 up and downregulated genes can be found in supplemental table 1. Interestingly, homeobox factor HoxD11 is in the top 5 most upregulated genes in hkPSCs. Homeobox transcription factors, which are important in anatomical patterning during development, showed hierarchical clustering when comparing bmMSCs with hkPSCs (Fig 3c). Homeobox paralogues Hox10 and Hox11 are important in kidney development.<sup>23,24</sup> Both genes are highly expressed in hkPSCs but not in bmMSCs, as confirmed by PCR (fig 3d). These results indicate that, although hkPSCs and bmMSCs may display a similar phenotype of surface markers, there are tissue specific differences in expression profile between the cell types.

### Immunomodulatory capacity of human kidney-derived perivascular stromal cells

One important and extensively studied feature of MSCs is their anti-inflammatory and immunomodulatory potential. MSCs are able to regulate proliferation and cytotoxicity of T cells, macrophages and B-cells which are also major players in kidney disease and transplantation, as reviewed elsewhere.<sup>25</sup> Therefore, we evaluated the immunomodulatory potential of hkPSCs in comparison to bmMSCs. Unstimulated human kPSCs and bmMSCs showed a similar expression profile for all major cytokines (Fig. 4a). We also evaluated the immunosuppressive capacity of hkPSCs. In a peripheral blood mononuclear cell (PBMC) suppression assay, where PBMCs were activated by polyclonal CD3/CD28 activation in the absence or presence of stromal cells, both hkPSCs and bmMSCs inhibited proliferation in a dose dependent manner (Fig 4b). However, bmMSCs were more potent in inhibiting proliferation at a lower cell ratio (8:1 PBMCs: MSC ratio) compared to hkPSCs.

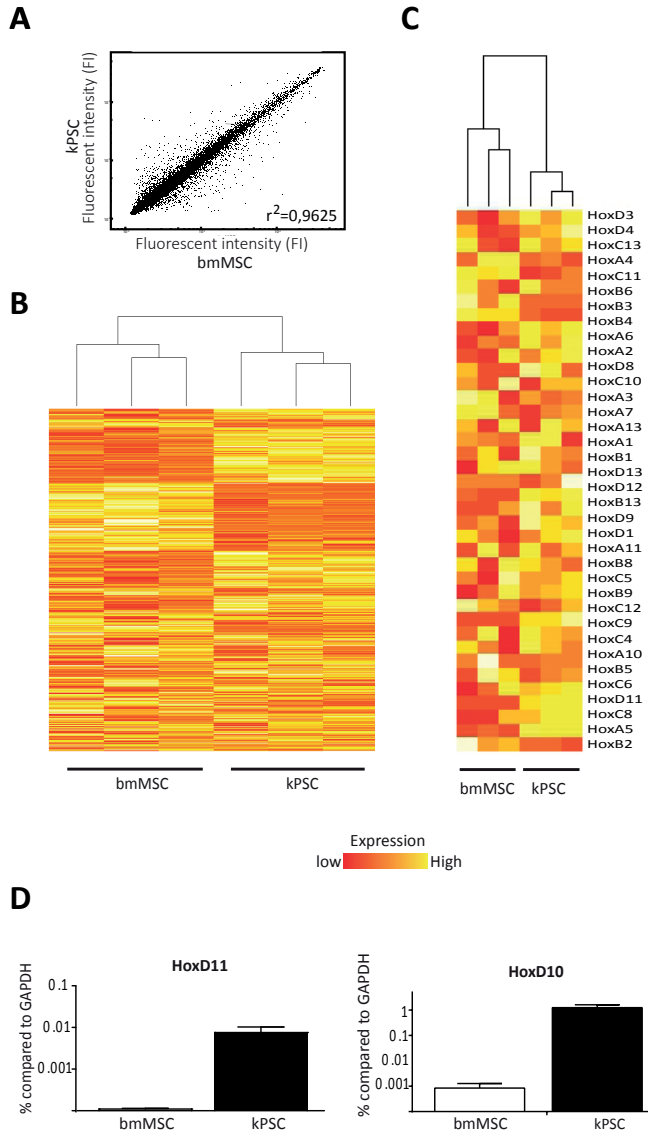


**Figure 3. Transcriptome analysis of human kPSCs compared to bmMSCs.** A) When comparing all transcripts (35000), bmMSCs and hkPSCs show a similar expression profile as depicted by a Pearson correlation score of 0.9625. B) hkPSCs and bmMSCs show an hierarchical clustering per cell type. C) Hierarchical clustering is also observed in Hox genes. D) Differential expression of HoxD11 and HoxD10, homeobox factors important for nephrogenesis, as confirmed by PCR. (GEO accession GSE77227, <http://www.ncbi.nlm.nih.gov/geo/query/acc.cgi?acc=GSE77227>) Abbreviations: BM-MSC, bone marrow derived mesenchymal stromal cells; GAPDH, glyceraldehyde-3-phosphate dehydrogenase; kPSC, kidney-derived perivascular stromal cells

Top 5 enriched genes kPSC						
Gene name	Symbol	Average signal bmMSC (SD)	Average signal kPSC (SD)	Fold increase	DiffScore	
endothelin 1	EDN1	206 (32)	2205 (238)	10,7	342,9	
tissue factor pathway inhibitor 2	TFPI2	329 (97)	3446 (609)	10,5	342,9	
regulator of G-protein signalling 4	RGS4	2500 (1282)	24091 (1615)	9,6	342,9	
homeobox D11	HOXD11	<200 (12)	1522 (109)	8,4	342,9	
myosin, heavy chain 10, non-muscle	MYH10	3322 (667)	21945 (1272)	6,6	342,9	
Top 5 enriched genes bmMSC						
Gene name	Symbol	Average signal bmMSC (SD)	Average signal kPSC (SD)	Fold increase	DiffScore	
latent transforming growth factor beta binding protein 2	LTBP2	7825 (449)	1818 (318)	-4,3	-340,5	
odd Oz/ten-m homolog 4	ODZ4	1745 (55)	482 (28)	-3,6	-340,5	
Htra serine peptidase 1	HTRA1	9384 (356)	2833 (621)	-3,3	-299,8	
fibronectin type III domain containing 1	FNDC1	12278 (1828)	189 (50)	-65,1	-256,5	
early B-cell factor 3	EBF3	931 (84)	273 (51)	-3,4	-243,2	

**Table 1. Top 5 differentially expressed genes comparing bmMSCs to hkPSCs.** Upper table: Increased gene expression in kPSC, sorted based on differential p-value. Lower table: upregulated genes in bmMSCs. Average signal for biological triplicates is shown. Only samples with a detection p-value<0.05 and a fluorescent intensity>200 (background levels) are shown. All differentially expressed genes show a significant p-value after correcting for multiple testing. Abbreviations: BM-MSCs, bone marrow-derived mesenchymal stromal cells; hkPSCs, human kidney-derived perivascular stromal cells.

### **Co-culture of endothelial cells with human kidney-derived perivascular stromal cells stabilizes vascular network formation**

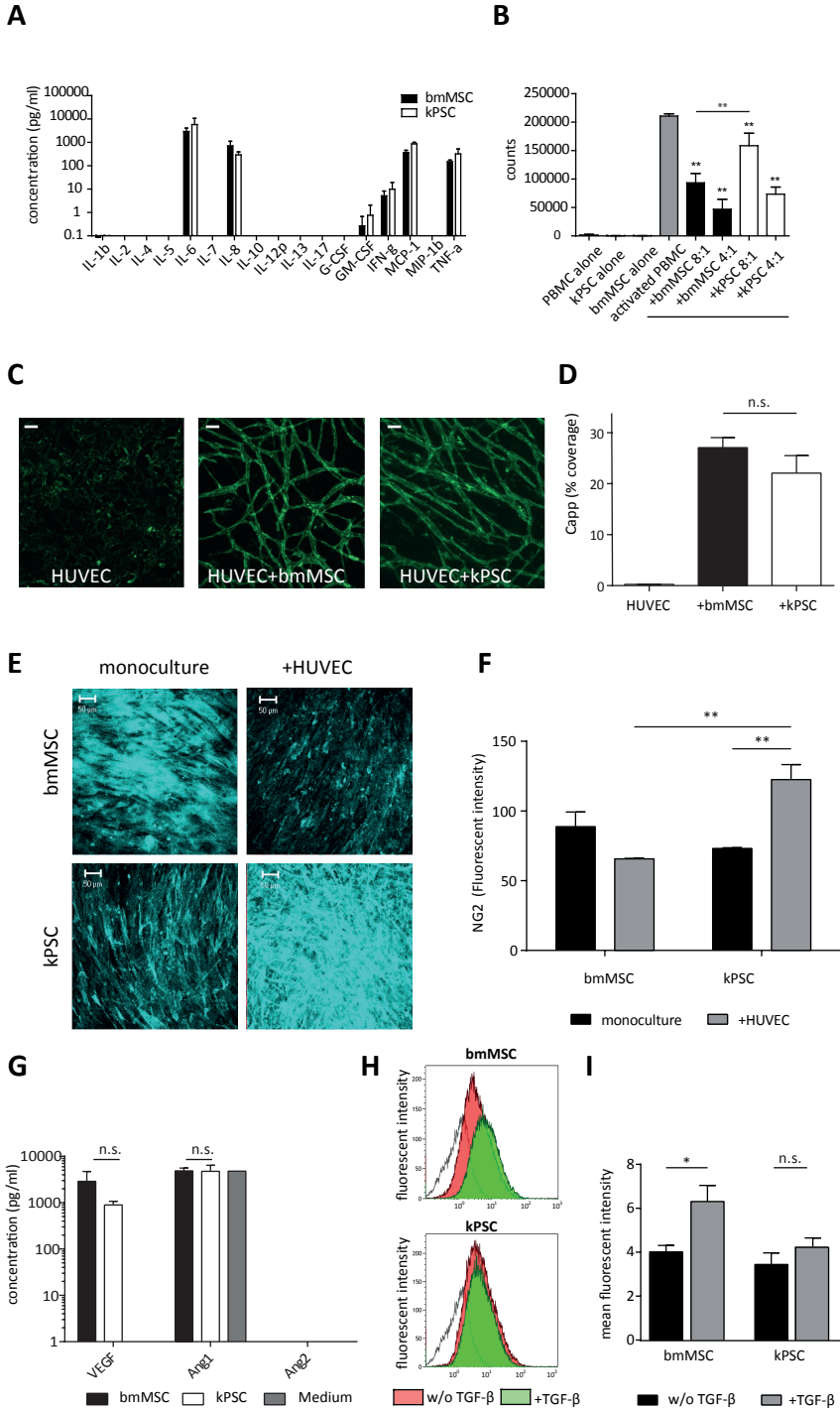
To evaluate whether cultured hkPSCs still have pericytic properties, cells were co-cultured with human umbilical vein endothelial cells (HUVEC). HUVECs were not able to form endothelial sprouts in monoculture. However, when co-cultured with either bmMSCs or hkPSCs, vascular plexus formation occurred (Fig 4c). There were no significant differences in vascular network formation between the cell types (Fig 4d). Interestingly, when cocultured with endothelial cells, hkPSCs showed an increase in NG2 expression while this was not observed with bmMSCs (Fig 4e,f). Both bmMSCs and hkPSCs mainly secreted Vascular Endothelial Growth Factor (VEGF) and there was no difference between the cell types in the levels of VEGF, angiopoetin 1 and angiopoetin 2 produced. (Fig 4g).

### **hkPSCs do not become myofibroblasts after stimulation with TGF- $\beta$**

As stromal cells in general have the capacity to become myofibroblasts after stimulation with TGF- $\beta$ , thereby contributing to fibrosis, we evaluated whether hkPSCs have this capacity. Interestingly, stimulation of hkPSCs with TGF- $\beta$  did not increase  $\alpha$ -SMA expression suggesting that hkPSCs did not become myofibroblasts (Fig 4 h,i).

### **Enhanced renal epithelial wound repair capacity of human kidney-derived perivascular stromal cells**

In order to evaluate the effect of hkPSCs on renal tubular epithelial repair, a scratch in a monolayer of human kidney proximal tubular epithelial cells (HK2) was made. Under control culture conditions, at least 28 hours was necessary for 80% wound closure. Interestingly, when conditioned media from hkPSCs was added, significant closure was already observed after 4 hours with 80% of the wound closed after 7 hours (mean of duplicate experiments from three different donors). Importantly, 14 hours was required to reach an 80% wound closure in parallel experiments with the conditioned media from bmMSCs, (Fig 5a,b). This shows that hkPSCs can produce factors able to better support renal epithelial repair. HGF is most likely an important factor in this activity as HGF was secreted at high levels by hkPSCs but not by bmMSCs whereas no differences were observed in the levels of other growth factors (PDGF-AA, PDGF-BB, endothelin1, FGF-a, FGF-B) (Fig 5c). Moreover, blocking the HGF-receptor on the epithelial cells resulted in a decreased wound healing. (Fig 5d,e)



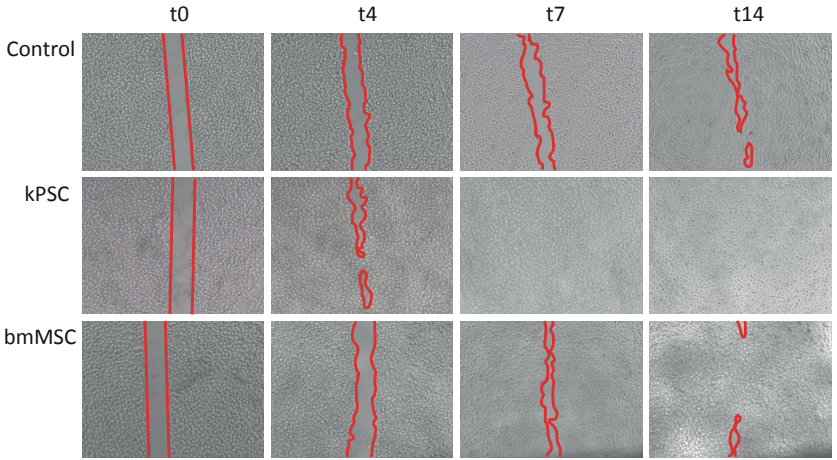
### Interstitial integration and survival of human kidney-derived perivascular stromal cells in the neonatal kidney

To determine the role of hkPSCs in kidney development, hkPSCs were injected into neonatal mice at postnatal day 1 using microinjection (Fig 6a,b). Interestingly, at day 4 post-injection, human kPSCs were able to integrate and survive within the cortical, but not the medullary interstitium of the mouse kidney with no evidence for rejection. (Fig. 6c). No such persistence was observed when human bmMSCs were injected (Fig 6d), consistent with our previous studies<sup>16</sup> No integration into tubular structures was seen with either human bmMSCs or hkPSCs upon injection. The persistence of viable human hkPSCs for 4 days within the renal interstitium suggests a differential integration capacity for this stromal cell type.

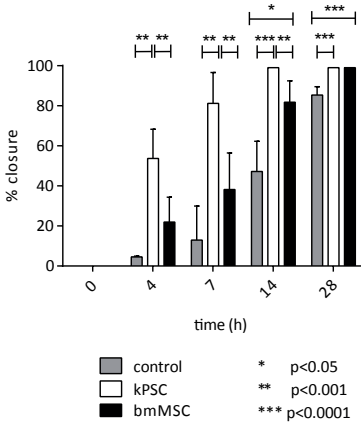
---

**Figure 4. Immunomodulatory and vascular stabilization function of hkPSCs** A) Cytokine expression profile of unstimulated human kPSCs and bmMSCs B) PBMC suppression assay. Proliferation of activated peripheral blood mononuclear cells (PBMCs) was decreased when cocultured with both hkPSCs and bmMSCs in a dose dependent matter. (ratio is number of activated PBMCs vs number of MSCs) C) When HUVECs are cocultured with either hkPSCs and bmMSCs endothelial networks were formed, which was not observed in monoculture. There were no significant differences in vascular plexus formation comparing coculture with bmMSCs or hkPSCs (D). E) When hkPSCs were cocultured with endothelial cells the expression of NG2 was increase; this was not seen with bmMSCs. F) Quantification of NG2 positivity with and without coculture with endothelial cells. G) No differences were observed in excretion of vascular growth factors by hkPSCs compared to bmMSCs. H) After stimulation of hkPSCs with 10 ng/ml TGF- $\beta$  there was no increase in  $\alpha$ -SMA expression. This was not observed for bmMSCs. White: isotype control, red: unstimulated cells, green: cells stimulated with 10ng/ml TGF- $\beta$  I) Quantification of  $\alpha$ -SMA positivity. n=3 biological triplicates. \*p<0.05, \*\* p<0.001, n.s. non-significant. Scale bar = 50  $\mu$ m (C, E). Abbreviations: Ang, angiopoietin; BM-MSC, bone marrow-derived mesenchymal stromal cells; G-CSF, granulocyte colony-stimulating factor; GM-CSF, granulocyte-macrophage colony-stimulating factor; HUVEC, human umbilical vein endothelial cells; IFN, interferon; IL, interleukin; kPSC, kidney-derived perivascular stromal cells; MIP-1, macrophage inflammatory protein 1; MCP-1, monocyte chemoattractant protein 1; n.s., nonsignificant; PBMC, peripheral blood mononuclear cells; TGF, transforming growth factor; TNF, tumor necrosis factor; VEGF, vascular endothelial growth factor; w/o, without.

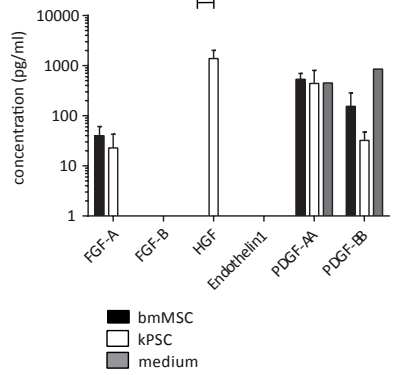
**A**



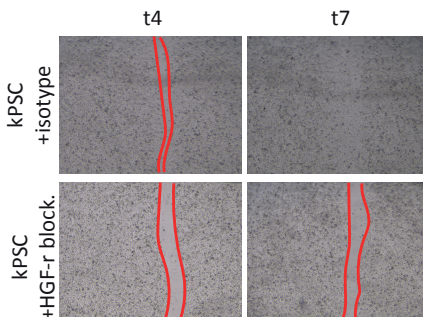
**B**



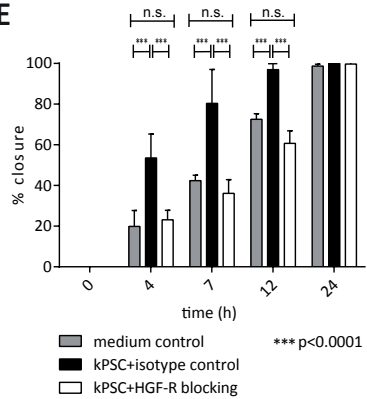
**C**



**D**



**E**

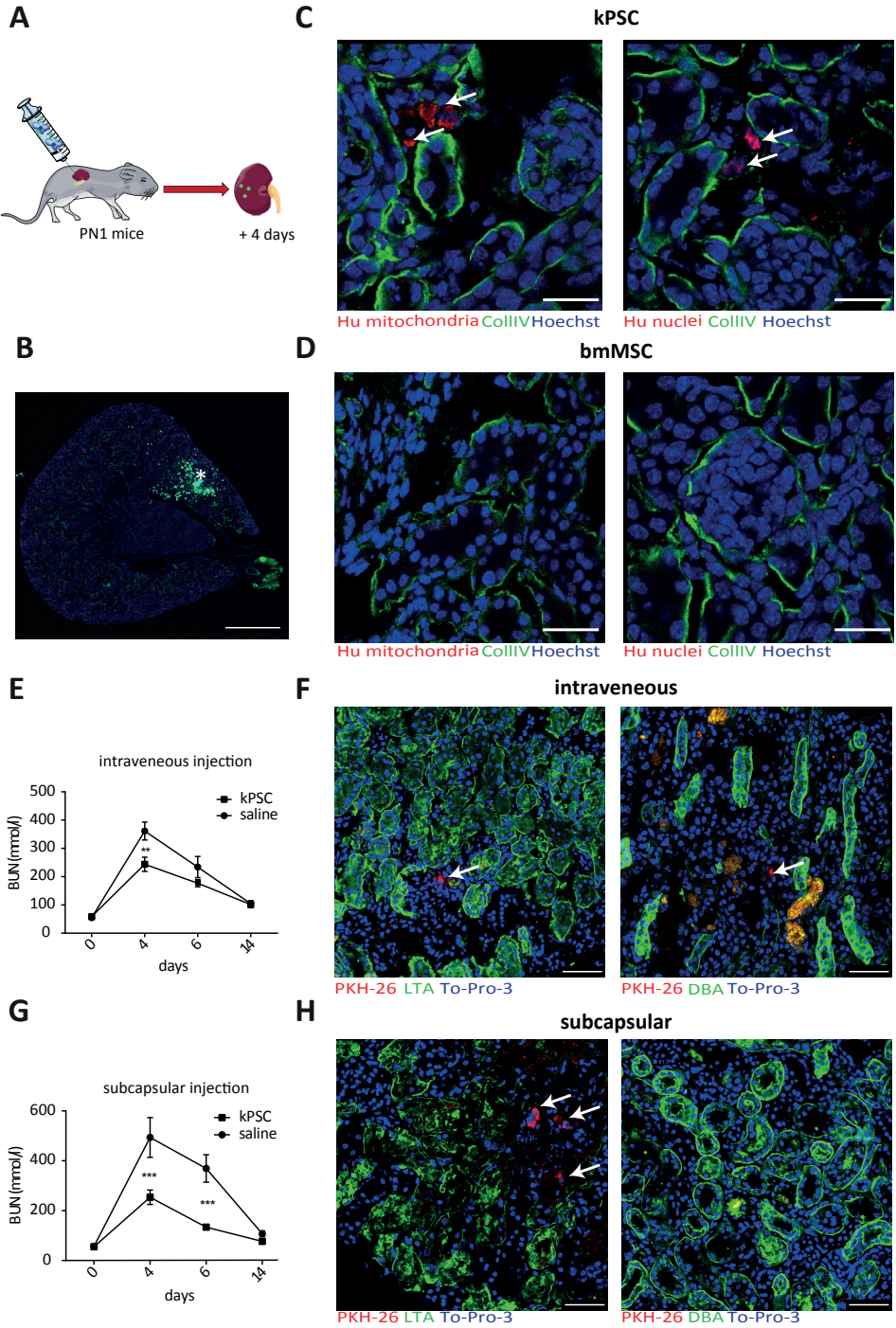


## Human kidney-derived perivascular stromal cells integrate in the renal interstitium and improve renal function in a glycerol-induced rhabdomyolysis acute kidney injury model

To access the effect of hkPSCs in kidney injury, we injected the cells in a glycerol-induced rhabdomyolysis acute kidney injury model. We evaluated the effect of hkPSCs via two routes of administration: renal subcapsular and intravenously. Blood Ureum Nitrogen (BUN) measurements show that, at the peak of acute kidney injury (AKI), renal function was significantly preserved in the hkPSC- treated group, independent of route of delivery (Fig 6 e,g). After both routes of delivery, interstitial integration of the PKH26-labelled hkPSCs was observed within the kidney, although less cells were observed after intravenous injection ( $0.0247 \pm 0.002$  cells/field subcapsular versus  $0.0164 \pm 0.0051$  cells/field i.v.). After subcapsular injection cells were mainly distributed in an area of  $990 \mu\text{m}$  around the area of injection. After intravenous injections cells most cells were observed in the medulla region and less in the cortex ( $0.0203 \pm 0.006$  vs.  $0.0095 \pm 0.0066$ ) (Fig 6 f,h).

---

**Figure 5. hkPSCs are able to enhance epithelial repair in a wound scratch assay.** A) Brightfield images showing representative images of the wound scratch assay in control medium or conditioned medium of hkPSCs and bmMSCs across a time period of 14 hours. B) Quantification of the rate of wound closure in all three conditions after 0, 4, 7, 14 and 28 hours. The wound closes significantly faster in the presence of hkPSC conditioned medium compared to bmMSC conditioned medium or control medium. C) Excretion of growth factors in the conditioned medium. HGF is excreted by hkPSCs but not by bmMSCs. D) Brightfield images showing representative images of the wound scratch assay with and without HGF-R blocking E) Quantification of the rate of wound closure after 0, 4, 7, 12 and 24 hours.  $n=3$  biological triplicates. \*  $p<0.05$ , \*\*  $p<0.001$ , \*\*\*  $p<0.0001$  Abbreviations: BM-MSC, bone marrow-derived mesenchymal stromal cell; FGF, fibroblast growth factor; HGF, hepatocyte growth factor; h, hour; kPSC, kidney-derived perivascular stromal cell; n.s., nonsignificant; PDGF, platelet-derived growth factor; t, time.



## Discussion

It has previously been reported that perivascular stromal cells from several different human organs share features with MSCs.<sup>10</sup> More recently it has been shown that organ derived perivascular cells may exhibit tissue-specific functions.<sup>26</sup> Human myocardial perivascular cells, for example, stimulate angiogenic responses under hypoxia and differentiate into cardiomyocytes *in vivo*; characteristics not seen in perivascular cells isolated from other tissues.<sup>27</sup>

Here we sought to isolate human kidney-derived perivascular stromal cells and show that these cells have distinct properties compared to human bmMSCs. In order to evaluate the functionality of these cells, their interaction with several different renal cell types, including endothelial cells, proximal tubular cells and (infiltrating) immune cells, was studied. There were similarities between human bmMSCs and hkPSCs, however, hkPSCs showed a distinct mRNA expression profile, did not differentiate into adipocytes and displayed a more potent kidney epithelial wound healing capacity. Furthermore, hkPSCs were able to integrate into the interstitium of the developing kidney, while bmMSCs did not. Finally, hkPSCs could preserve kidney function in a glycerol-induced rhabdomyolysis model of acute kidney injury.

---

**Figure 6. hkPSCs are able to survive and integrate into the kidney interstitium in a neonatal injection method and in a model of AKI and gave preservation of renal function.** A) Cells and fluorescent microspheres were injected into the kidney of neonatal mice (PND1). B) Injection into the kidney was confirmed by fluorescent microspheric beads (\*). C) hkPSCs injected into the kidneys of neonatal mice (PND1) were localized in the cortical interstitium as shown with specific antibodies for human mitochondria and human nuclei respectively (arrows). D) No bmMSCs could be found in the kidney 4 days after injection. E) Blood Ureum Nitrogen (BUN) measurements after i.v. injection of hkPSCs in a glycerol-induced rhabdomyolysis model. F) hkPSCs were localized mainly in the interstitium of the medulla after i.v. infusion and did not integrate in the LTA positive proximal tubuli or DBA positive collection duct. G) BUN after subcapsular administration of hkPSCs in a glycerol-induced rhabdomyolysis model. H) hkPSCs integrated in the interstitium in the cortex and not in the medulla. No integration in the tubuli was observed. Scale bars = 500  $\mu$ m (B) and 50  $\mu$ m (C, D, F, H). Abbreviations: BM-MSC, bone marrow-derived mesenchymal stromal cell; BUN, blood ureum nitrogen; kPSC, kidney-derived perivascular stromal cell.

As there is a lack of specific markers of MSCs, the ISCT has proposed criteria to define MSC's. These include plastic adherence, the marker expression of CD73, CD90 and CD105 while being negative for CD14, CD34 and CD45 and the capacity to differentiate into bone, cartilage and fat *in vitro*<sup>1</sup>. The hkPSCs we isolated did not fulfill these criteria as there was no adipocyte differentiation. However, these criteria are based on bone marrow-derived MSCs and the lack of this capacity might actually be beneficial as it has previously been shown that MSCs injected into the renal artery in a glomerulonephritis model can turn into adipocytes in the glomeruli accompanied by glomerular sclerosis around these adipocytes.<sup>28</sup>

MSCs are important for tissue homeostasis most likely via the secretion of several soluble factors and microvesicles containing amongst others mRNAs and miRNAs.<sup>29,30</sup> Indeed, bmMSC-conditioned medium is able to accelerate wound healing *in vitro*.<sup>31,32</sup> and in a mouse model of glycerol induced acute kidney injury, enhanced recovery in kidney function was observed when either MSCs or MSC-derived microvesicles were injected.<sup>29</sup> The same is most likely true for organ-derived perivascular stromal cells. Conditioned medium from murine kidney MSC-like cells was able to enhance kidney epithelial wound healing in an *in vitro* wound scratch assay.<sup>16</sup> Here we show that the conditioned medium from human kPSCs elicited accelerated repair in a tubular epithelial wound scratch assay, suggesting tissue-specific paracrine signaling. An important factor in this signaling is most likely hepatic growth factor (HGF) as HGF is highly secreted by kPSCs and not by bmMSCs. Moreover, after blocking of the HGF-receptor the effect of hkPSCs on wound healing was diminished. HGF has long been recognized as an important factor in kidney regeneration and attenuation of renal fibrosis in several different animal models.<sup>33</sup> HGF is primarily produced in non-epithelial cells, such as fibroblasts and pericytes, and is able to block myofibroblast activation and therefore renal fibrosis. Moreover, HGF can prevent tubular epithelial cell death both *in vitro* and *in vivo*, the latter resulting in improved renal function after acute kidney injury.<sup>34-36</sup> HGF is most likely also important in human kidney regeneration as a high expression of HGF in protocol biopsies after kidney transplantation correlated with lower levels of fibrosis.<sup>37</sup>

While this study is not the first to describe an MSC-like population in the human kidney<sup>38</sup>, hkPSCs isolated through the current protocol represent a distinct population. Resident kidney MSCs as described by Bruno et al.<sup>38</sup> were isolated from the glomeruli whereas the hkPSCs described in the current protocol were isolated based on NG2 expression. As NG2 is mainly expressed around the large vessels (fig 1a), this is more likely to represent a different perivascular

population. Another major difference is that hkPSCs are not positive for CD24, Pax2, Oct4 or NANOG (supplementary fig. 1) and are, in contrast to glomerular MSCs, not able to differentiate into adipocytes.

The differences between human kPSCs and bmMSCs mentioned above may reflect differences in imprinting by the tissue of origin. This was previously also observed for fibroblasts isolated from different organs.<sup>39</sup> In the current study, the expression profile of homeobox genes, which are important for anatomical patterning, showed a differential upregulation of HoxD10 and HoxD11 expression by hKPC with the latter gene in the top 5 most differentially expressed genes. Both Hox10 and Hox11 are crucial for nephrogenesis. Hox10 genes function in the differentiation and integration of the FoxD1<sup>+</sup> renal cortical stroma while Hox11 genes are expressed in the metanephric mesenchyme. Loss of either Hox10 or Hox11 gene function results in the loss of ureteric bud induction, reduced branching and decreased nephrogenesis; phenotypes only described for Hox10 and 11 mutants and not for other Hox mutants.<sup>23,24</sup> This potential tissue 'memory of origin' may be reflected in the observed differences in potential to integrate back into the kidney when injected into the renal parenchyma. Such integration was never observed for the bone marrow MSCs, while the hkPSCs migrated into the renal interstitium and survived. While we observed integration into the cortical interstitial compartment, we did not observe any integration into the epithelium. Previously, it was reported that murine kidney-derived MSC like cells can integrate into the developing collecting duct. However, the human kPSCs were isolated from the perivascular fraction based on NG2 expression, while Li. et al isolated murine MSC-like cells based on HoxB7 expression and thus the collecting duct epithelial compartment<sup>16</sup>. When looking at the expression pattern of the homeobox factors, HoxB7 expression in the human kPSCs was low, while HoxD11 expression was high, suggesting a different origin likely reflected in their distinct integration capacity and function. It remains possible that a human kidney MSC-like population similar to that isolated from mouse or reciprocally a murine kPSC population similar to the hkPSC described here may exist.

Interestingly, hkPSCs were able to integrate back into the renal interstitium and reduce the severity of kidney injury *in vivo* in a rhabdomyolysis model. This was independent of the route of delivery as both subcapsular and intravenous injected hkPSCs were able to preserve renal function. However, with the subcapsular injections integration of the hkPSCs into the interstitium appeared more pronounced as did the reno-protective effect.

Whether human kPSCs are more suitable for cell therapy for kidney diseases compared to bmMSCs, which are currently studied in clinical trials, still remains to be further elucidated. Their capacity to reintegrate into the renal stroma, to improve tubular epithelial wound repair

and to preserve function in an AKI model would suggest that hkPSCs may have an organotypic role in maintaining and restoring renal interstitial homeostasis without showing the risk of increasing fibrosis. To be able to compare these cell types for future cell therapy purposes we chose to isolate the hkPSCs with a standard operation procedure (SOP) in a clinical grade manner, with clinical grade enzymes, materials and methods which would allow direct translation into a clinical product. Using this protocol, large quantities of clinical grade isolated hkPSCs can be obtained. The yield from one human kidney would be an average of  $2.7 \times 10^{12}$  hkPSCs after passage 6. Hence, one donor kidney could yield sufficient number of hkPSCs for the treatment of several different patients as a cell therapy. This makes human kPSCs an interesting new cell source to develop for regenerative medicine for kidney diseases.

## Conclusions

These data show that human kPSCs show distinct functional properties compared to bmMSCs with respect to growth factor excretion, interstitial integration and amelioration of kidney injury, suggesting significant potential for hkPSCs and/or their secretome as therapeutic candidates for the treatment of kidney disease.

## Acknowledgements

The research leading to these results has received funding from the European Community's Seventh Framework Program (FP7/2007-2013) under grant agreement number 305436 (STELLAR), the National Health and Medical Research Council (ID1054985) and Kidney Health Australia ML is an NHMRC Senior Principal Research Fellow. We thank J.M.G.J.Duijs and A.M. van Oeveren-Rietdijk for their technical support.

## References

- 1 Dominici, M. *et al.* Minimal criteria for defining multipotent mesenchymal stromal cells. The International Society for Cellular Therapy position statement. *Cytotherapy*. **8** (4), 315-317, doi:Q2183N8UT042W62H [pii]10.1080/14653240600855905, (2006).
- 2 Pittenger, M. F. *et al.* Multilineage potential of adult human mesenchymal stem cells. *Science*. **284** (5411), 143-147 (1999).
- 3 Morigi, M. *et al.* Human bone marrow mesenchymal stem cells accelerate recovery of acute renal injury and prolong survival in mice. *Stem Cells*. **26** (8), 2075-2082, doi:2007-0795 [pii]10.1634/stemcells.2007-0795, (2008).
- 4 Wang, Y., He, J., Pei, X. & Zhao, W. Systematic review and meta-analysis of mesenchymal stem/stromal cells therapy for impaired renal function in small animal models. *Nephrology (Carlton)*. **18** (3), 201-208, doi:10.1111/nep.12018, (2013).
- 5 Casiraghi, F. *et al.* Localization of Mesenchymal Stromal Cells Dictates Their Immune or Proinflammatory Effects in Kidney Transplantation. *Am J Transplant*. **12** 2373-2383 (2012).
- 6 Perico, N. *et al.* Autologous mesenchymal stromal cells and kidney transplantation: a pilot study of safety and clinical feasibility. *Clin J Am Soc Nephrol*. **6** (2), 412-422 (2011).
- 7 Tan, J. *et al.* Induction therapy with autologous mesenchymal stem cells in living-related kidney transplants: a randomized controlled trial. *JAMA*. **307** (11), 1169-1177, doi:10.1001/jama.2012.316307/11/1169 [pii], (2012).
- 8 Perico, N. *et al.* Mesenchymal stromal cells and kidney transplantation: pretransplant infusion protects from graft dysfunction while fostering immunoregulation. *Transpl Int*. **26** (9), 867-878, doi:10.1111/tri.12132, (2013).
- 9 Reinders, M. E. *et al.* Autologous bone marrow-derived mesenchymal stromal cells for the treatment of allograft rejection after renal transplantation: results of a phase I study. *Stem Cells Transl Med*. **2** (2), 107-111, doi:10.5966/sctm.2012-0114sctm.2012-0114 [pii], (2013).
- 10 Crisan, M. *et al.* A perivascular origin for mesenchymal stem cells in multiple human organs. *Cell Stem Cell*. **3** (3), 301-313 (2008).
- 11 Rabelink, T. J. & Little, M. H. Stromal cells in tissue homeostasis: balancing regeneration and fibrosis. *Nat Rev Nephrol*. **9** (12), 747-753, doi:10.1038/nrneph.2013.152, (2013).
- 12 Dekel, B. *et al.* Isolation and characterization of nontubular sca-1+lin- multipotent stem/progenitor cells from adult mouse kidney. *J Am Soc Nephrol*. **17** (12), 3300-3314, doi:10.1681/ASN.2005020195, (2006).
- 13 Huang, Y. *et al.* Kidney-derived stromal cells modulate dendritic and T cell responses. *J Am Soc Nephrol*. **20** (4), 831-841, doi:10.1681/ASN.2008030310, (2009).
- 14 Huang, Y. *et al.* Kidney-derived mesenchymal stromal cells modulate dendritic cell function to suppress alloimmune responses and delay allograft rejection. *Transplantation*. **90** (12), 1307-1311, doi:10.1097/TP.0b013e3181fdd9eb, (2010).
- 15 Pelekanos, R. A. *et al.* Comprehensive transcriptome and immunophenotype analysis of renal and cardiac MSC-like populations supports strong congruence with bone marrow MSC despite maintenance of distinct identities. *Stem Cell Res*. **8** (1), 58-73, doi:10.1016/j.scr.2011.08.003S1873-5061(11)00109-7 [pii], (2012).
- 16 Li, J. *et al.* Collecting duct-derived cells display mesenchymal stem cell properties and retain selective in vitro and in vivo epithelial capacity. *J Am Soc Nephrol*. **26** (1), 81-94, doi:10.1681/asn.2013050517, (2015).

- 17 Jaffe, E. A., Nachman, R. L., Becker, C. G. & Minick, C. R. Culture of human endothelial cells derived from umbilical veins. Identification by morphologic and immunologic criteria. *J Clin Invest.* **52** (11), 2745-2756, doi:10.1172/jci107470, (1973).
- 18 Orlova, V. V. *et al.* Generation, expansion and functional analysis of endothelial cells and pericytes derived from human pluripotent stem cells. *Nat Protoc.* **9** (6), 1514-1531, doi:10.1038/nprot.2014.102, (2014).
- 19 Angelotti, M. L. *et al.* Characterization of renal progenitors committed toward tubular lineage and their regenerative potential in renal tubular injury. *Stem Cells.* **30** (8), 1714-1725, doi:10.1002/stem.1130, (2012).
- 20 Nijhoff, M. F. *et al.* Glycemic Stability Through Islet-After-Kidney Transplantation Using an Alemtuzumab-Based Induction Regimen and Long-Term Triple-Maintenance Immunosuppression. *Am J Transplant.* doi:10.1111/ajt.13425, (2015).
- 21 Ozerdem, U., Grako, K. A., Dahlin-Huppe, K., Monosov, E. & Stallcup, W. B. NG2 proteoglycan is expressed exclusively by mural cells during vascular morphogenesis. *Dev Dyn.* **222** (2), 218-227, doi:10.1002/dvdy.1200, (2001).
- 22 Watson, J. T. *et al.* CD271 as a marker for mesenchymal stem cells in bone marrow versus umbilical cord blood. *Cells Tissues Organs.* **197** (6), 496-504, doi:10.1159/000348794, (2013).
- 23 Wellik, D. M., Hawkes, P. J. & Capecchi, M. R. Hox11 paralogous genes are essential for metanephric kidney induction. *Genes Dev.* **16** (11), 1423-1432, doi:10.1101/gad.993302, (2002).
- 24 Yallowitz, A. R., Hrycaj, S. M., Short, K. M., Smyth, I. M. & Wellik, D. M. Hox10 genes function in kidney development in the differentiation and integration of the cortical stroma. *PLoS One.* **6** (8), e23410, doi:10.1371/journal.pone.0023410, (2011).
- 25 Leuning, D. G., Reinders, M. E., de Fijter, J. W. & Rabelink, T. J. Clinical translation of multipotent mesenchymal stromal cells in transplantation. *Semin Nephrol.* **34** (4), 351-364, doi:10.1016/j.semnephrol.2014.06.002, (2014).
- 26 Sacchetti, B. *et al.* No Identical "Mesenchymal Stem Cells" at Different Times and Sites: Human Committed Progenitors of Distinct Origin and Differentiation Potential Are Incorporated as Adventitial Cells in Microvessels. *Stem Cell Reports.* **6** (6), 897-913, doi:10.1016/j.stemcr.2016.05.011, (2016).
- 27 Chen, W. C. *et al.* Human myocardial pericytes: multipotent mesodermal precursors exhibiting cardiac specificity. *Stem Cells.* **33** (2), 557-573, doi:10.1002/stem.1868, (2015).
- 28 Kunter, U. *et al.* Mesenchymal stem cells prevent progressive experimental renal failure but maldifferentiate into glomerular adipocytes. *J Am Soc Nephrol.* **18** (6), 1754-1764, doi:10.1681/asn.2007010044, (2007).
- 29 Bruno, S. *et al.* Mesenchymal stem cell-derived microvesicles protect against acute tubular injury. *J Am Soc Nephrol.* **20** (5), 1053-1067, doi:10.1681/ASN.2008070798ASN.2008070798 [pii], (2009).
- 30 Lindoso, R. S. *et al.* Extracellular vesicles released from mesenchymal stromal cells modulate miRNA in renal tubular cells and inhibit ATP depletion injury. *Stem Cells Dev.* **23** (15), 1809-1819, doi:10.1089/scd.2013.0618, (2014).
- 31 Smith, A. N. *et al.* Mesenchymal stem cells induce dermal fibroblast responses to injury. *Exp Cell Res.* **316** (1), 48-54, doi:10.1016/j.yexcr.2009.08.001, (2010).
- 32 Walter, M. N., Wright, K. T., Fuller, H. R., MacNeil, S. & Johnson, W. E. Mesenchymal stem cell-conditioned medium accelerates skin wound healing: an in vitro study of fibroblast and keratinocyte scratch assays. *Exp Cell Res.* **316** (7), 1271-1281, doi:10.1016/j.yexcr.2010.02.026, (2010).

- 33 Liu, Y. Hepatocyte growth factor in kidney fibrosis: therapeutic potential and mechanisms of action. *Am J Physiol Renal Physiol.* **287** (1), F7-16, doi:10.1152/ajprenal.00451.2003, (2004).
- 34 Frei, U. *et al.* Acute rejection in low-toxicity regimens: clinical impact and risk factors in the Symphony study. *Clin Transplant.* **24** (4), 500-509, doi:10.1111/j.1399-0012.2009.01093.x, (2010).
- 35 Gao, X. *et al.* Hepatocyte growth factor gene therapy retards the progression of chronic obstructive nephropathy. *Kidney Int.* **62** (4), 1238-1248, doi:10.1111/j.1523-1755.2002.kid579.x, (2002).
- 36 Dai, C., Yang, J. & Liu, Y. Single injection of naked plasmid encoding hepatocyte growth factor prevents cell death and ameliorates acute renal failure in mice. *J Am Soc Nephrol.* **13** (2), 411-422 (2002).
- 37 Kellenberger, T., Marcussen, N., Nyengaard, J. R., Wogensen, L. & Jespersen, B. Expression of hypoxia-inducible factor-1alpha and hepatocyte growth factor in development of fibrosis in the transplanted kidney. *Transpl Int.* **28** (2), 180-190, doi:10.1111/tri.12475, (2015).
- 38 Bruno, S. *et al.* Isolation and characterization of resident mesenchymal stem cells in human glomeruli. *Stem Cells Dev.* **18** (6), 867-880, doi:10.1089/scd.2008.0320, (2009).
- 39 Chang, H. Y. *et al.* Diversity, topographic differentiation, and positional memory in human fibroblasts. *Proc Natl Acad Sci U S A.* **99** (20), 12877-12882, doi:10.1073/pnas.162488599, (2002).

Video available

